Exciton Dissociation

DOI: 10.1002/anie.201402568

Organic Photovoltaics: Elucidating the Ultra-Fast Exciton Dissociation Mechanism in Disordered Materials**

Henry M. Heitzer, Brett M. Savoie, Tobin J. Marks, and Mark A. Ratner**

Abstract: *Organic photovoltaics (OPVs) offer the opportunity for cheap, lightweight and mass-producible devices. However, an incomplete understanding of the charge generation process, in particular the timescale of dynamics and role of exciton diffusion, has slowed further progress in the field. We report a new Kinetic Monte Carlo model for the exciton dissociation mechanism in OPVs that addresses the origin of ultra-fast (< 1 ps) dissociation by incorporating exciton delocalization. The model reproduces experimental results, such as the diminished rapid dissociation with increasing domain size, and also lends insight into the interplay between mixed domains, domain geometry, and exciton delocalization. Additionally, the model addresses the recent dispute on the origin of ultra-fast exciton dissociation by comparing the effects of exciton delocalization and impure domains on the photodynamics.This model provides insight into exciton dynamics that can advance our understanding of OPV structure–function relationships.*

The prospect of ultra-thin, mechanically flexible, mass-producible, and low-cost solar cells has stimulated much research in organic photovoltaics (OPVs). While significant progress has been made in understanding OPV structure–function relationships, important questions remain pertaining to the fundamental chemistry and physics underlying their operation. In the conventional description, photoexcitations rapidly thermalize into spatially confined electron–hole pairs (excitons). These excitons are strongly bound due to the low dielectric constants of typical organic materials, making it energetically demanding to split into constituent electrons and holes—the first requisite step for photocurrent generation.[1,2] Introducing a complementary material with a sufficiently high electron affinity (acceptor) for electron transfer, or low ionization potential (donor) for hole transfer, enables efficient conversion of excitons into charge-separated species (exciton dissociation), with the hole residing in the donor phase and the electron in the acceptor phase.[3,4] In this model, excitons sample the OPV active layer volume as diffusing, point-like species, and the timescale of exciton conversion to separated charges is limited solely by the time required for excitons to diffuse to a donor–acceptor interface (heterojunction).[5,6] In this contribution, we propose a new model incorporating initial exciton delocalization that explains recent experimental findings of ultra-fast exciton dissociation that cannot be reconciled by previous models.

Until recently, prevailing theories of exciton dissociation postulated that molecular excitons hop randomly from one site to another via Förster energy transfer.[7,8] This view was strongly informed by early work on vapor-deposited bilayer OPVs. In bilayer OPVs, limited exciton diffusion leads to incomplete exciton dissociation, low photocurrent production, and modest power conversion efficiencies of ca. 1 %.[3,4,9–11] This microstructure differs substantially from the smaller bicontinuous domains (< 20 nm) of active layers found in high-efficiency bulk heterojunction (BHJ) polymeric devices.[12–14] Bulk heterojunction structures offer the advantage that excitons need diffuse only a short distance (10–20 nm) before reaching a heterojunction. Small domains ensure that excitons reach donor–acceptor interfaces before recombining, leading to higher densities of mobile free charges and ultimately, enhanced OPV performance.

Given the small domain sizes of typical BHJ active layers, fairly rapid exciton dissociation might be expected. However, recent studies show that the majority of excitons are dissociated within 1 ps of excitation in efficient BHJ systems[15,16]—far more rapidly than would be consistent with simple point-like diffusion, even involving small domains. Ultra-fast dissociation, on timescales competitive with exciton localization, calls into question the validity of assuming localized excitons as the reference state for understanding the dynamics. These observations recently led some groups to hypothesize that exciton delocalization may explain the timescale of dissociation.[17,18] If the initial state is delocalized (Wannier exciton) (illustrated in Figure 1 A below), this would reconcile the dissociation timescale with the donor and acceptor phase dimensions in BHJ cell active layers. The delocalization hypothesis is also supported by spectroscopic observations of coherent exciton diffusion[19] and photoemission,[20] that suggest the timescale for exciton localization may be slower than previously thought.

In contrast to the above delocalization picture, it is also possible to describe the timescale of exciton dissociation by simply considering that the donor and acceptor phases are

[*] H. M. Heitzer, B. M. Savoie, Prof. T. J. Marks, Prof. M. A. Ratner
Department of Chemistry, the Materials Research Center, and the the Argonne-Northwestern Solar Energy Research Center, Northwestern University
Evanston, IL, 60208 (USA)
E-mail: t-Marks@northwestern.edu
ratner@northwestern.edu

[**] This work is supported as part of the ANSER Center, an Energy Frontier Research Center funded by the U.S. Department of Energy, Office of Science, and Office of Basic Energy Sciences under Award Number DE-SC0001059. H.M.H. is supported by the Dept. of Defense (DoD) through the National Defense Science & Engineering Graduate Fellowship (NDSEG) Program, and B.M.S. by the Northwestern MRSEC (NSF DMR-1121262) through a graduate fellowship.

Supporting information for this article is available on the WWW under http://dx.doi.org/10.1002/anie.201402568.

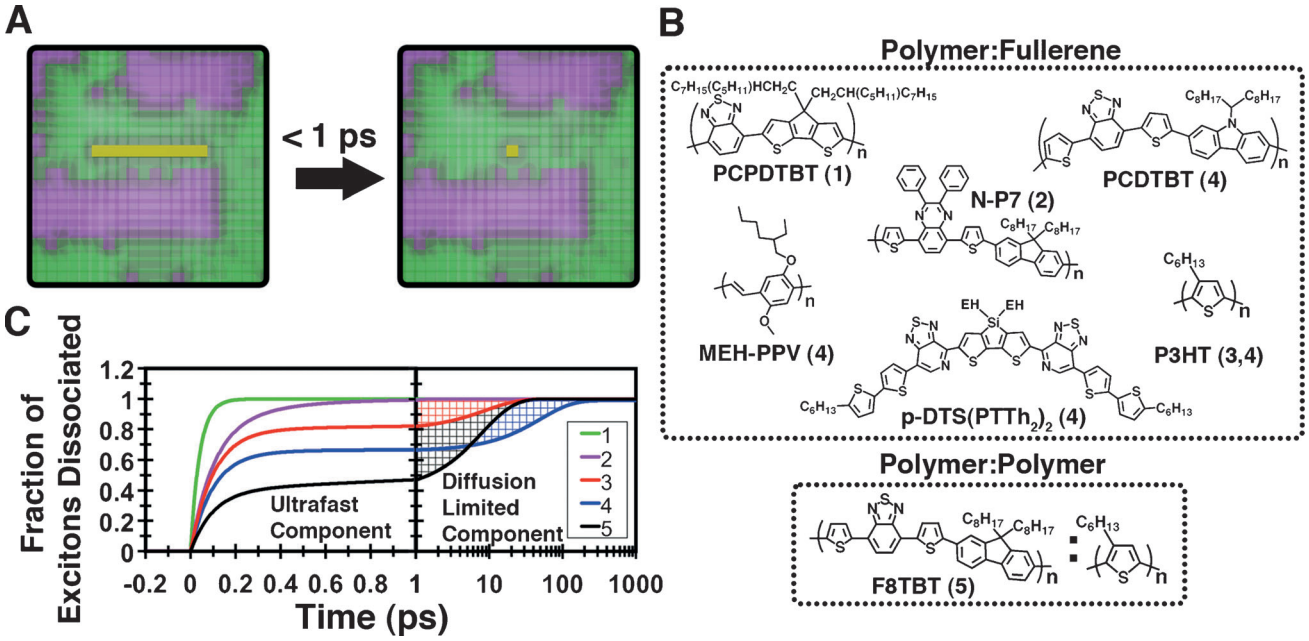

Figure 1. A) Schematic depiction of exciton localization processes in a BHJ phase with donor (green) and acceptor (purple) domain sizes = 10 nm. Left: exciton (yellow line) delocalized over multiple donor sites upon initial excitation. Right: after 1 ps the exciton localizes to one site. B) Structures of bulk-heterojunction components investigated here. C) Exponential kinetic fits extracted from transient absorption data at low laser fluence ($< 10\ \mu J\ cm^{-2}$).[15–17,21,22] Fraction of excitons dissociated is represented by the rise of cation signal as measured experimentally in the donor materials. The spectra show both the ultra-fast and diffusion-limited generation of cations in polymer:fullerene and polymer:polymer blends. Low laser fluences are important since exciton–exciton annihilation in the donor material at high laser intensities can mask the diffusion-limited component. Labeling of samples **1–5** is based upon domain sizes of each system, with **1** being the smallest and **5** being the largest. There are two data sets for P3HT (samples 3 and 4) corresponding to two different experimental studies.

impure. For instance, recent morphological studies have identified the presence of mixed phases, regions of the active layer marked by disorder and molecular mixing of the donor and acceptor materials.[23,24] The generality of pure domains has been questioned, with mounting evidence that typical fullerene acceptors are miscible to some degree with various donors. Separate studies have established that in some blends pure phases are absent, with acceptor molecules intercalating with donor phases at densities of up to 30% by volume.[25,26]

To date, no model describing the coexistence of ultra-fast and diffusion-limited exciton dissociation has been available. Here we present a new model that reproduces the experimental fractions of ultra-fast and diffusion-limited dissociation, by combining initial exciton delocalization with subsequent exciton localization and diffusive hopping. Using this model, we then examine the contrasting mechanisms for ultra-fast dissociation, and initial delocalization, versus impure domain-mediated dissociation. We employ kinetic data from several published low-intensity transient absorption studies to serve as a reference for our simulations (Figure 1C). This dataset includes several donor polymers and a high-performing small-molecule donor, all blended with fullerenes, in addition to a polymer:polymer BHJ system (Figure 1B).[15,16,18,22,23] Each kinetic trace reveals an ultrafast component that is limited by the instrumental response of the particular experimental setup. The slower component (picosecond rise time) is interpreted to be diffusion-limited, and its magnitude increases with the degree of blend phase segregation. For example, PCPDTBT:$PC_{60}BM$ system **1** is highly mixed when spin-cast without processing additives. In contrast, annealed P3HT:$PC_{60}BM$ films undergo phase segregation, as do F8TBT:P3HT blends, coinciding with larger diffusion-limited spectral components.

The Kinetic Monte Carlo[27] formalism, which has been used extensively to model hopping regime transport,[28] is used here to model exciton diffusion in BHJ donor materials. Diffusion is modeled by assuming excitons hop from site to site with an experimentally determined rate. A donor site is chosen at random as the excitation site, and the exciton is initially ($t_0 = 0$) delocalized a variable distance d over the x-axis, which represents the donor backbone (Figure 1A). While excitons are only generated on the donor sites in this study, the results are also relevant to charge generation in the acceptor (fullerene) domains. Extended conjugation enables delocalization of the initial excited states along the conjugated backbone.[29] Delocalization can vary from a few Å to μm,[20] depending on the chemical composition, purity, macromolecular planarity, and order of the material.[30–32] While excited state delocalization can be extensive, it is often short-lived, typically localizing to small areas in less than 1 ps.[31] In the present model, it is assumed that if any portion of the initially delocalized exciton reaches an interface, it undergoes dissociation. After the first exciton hop, at time step > 1 ps, the exciton is localized (Figure 1A) on one donor site ($d =$ 1 nm) and then diffuses to neighboring donor sites by Förster energy transfer.[33] The localized (Frenkel) exciton proceeds to diffuse via Förster energy transfer until it either reaches

a donor–acceptor interface, or recombines. At the beginning of each simulation, a recombination time, t_r, is chosen from a Gaussian distribution centered on the experimental recombination rate, r_r, of an exciton in the well-characterized donor polymer poly(3-hexylthiophene) (P3HT). If the simulation reaches t_r, then the exciton will recombine. A more detailed description of the model and parameter values is given in the Supporting Information.

The heterojunction is modeled site-wise with equal proportions of donor and acceptor sites. The sites are placed on a 3D cubic lattice with periodic boundary conditions in all directions. Each site is assumed to be 1 nm^3 in size, and there are 30 sites in each direction ($x,y,z = 30$ nm with 27000 total sites). The exciton has a weighted diffusion rate along each axis corresponding to different hopping rates along the backbone (x-axis), π stacking direction (z-axis), and lamellar dimension (y-axis).[34] In the present analysis, the Ising method is used to generate domains on the 3D cubic lattice (for more information on the method and specific parameters used, see the Supporting Information).[35] This method can produce morphologies that simulate both mixed and pure domains (Figure 2). By running simulations over many morphologies, morphological contributions to the exciton dynamics can be stochastically examined.

Domain sizes are chosen to be 5, 10, 15, and 20 nm which are considered relevant to these devices (Figure 2).[36,37] Additionally, dispersed domains are modeled to capture the behavior in systems with disordered domains. For each domain size the excitons are assigned varying initial degrees of delocalization, d, 1, 5, and 10 nm. The delocalization lengths are chosen to correspond to different reported values of the delocalization for various materials and processing conditions.[19,38,39] Each data set represents 10000 simulations per morphology over 10 different morphologies.

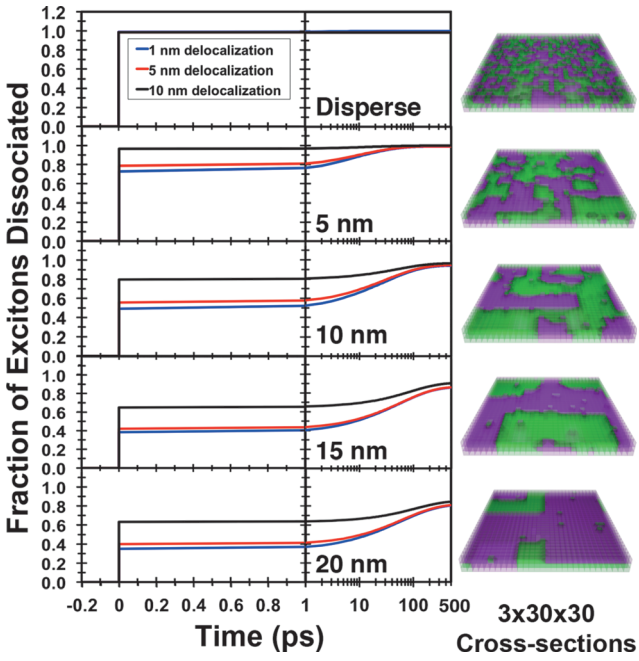

Figure 2. Predicted exciton dissociation for varying donor (green) and acceptor (purple) BHJ domain sizes (dispersed, 5 nm, 10 nm, 15 nm, and 20 nm) and varied initial delocalization of 1 nm (blue), 5 nm (red), and 10 nm (black). A representative morphology image for each domain is shown on the right using 3 layers from a lattice. Note that in all morphologies there is an equal amount of donor and acceptor material. Each data set represents 10 different morphologies generated using the Ising algorithm for a given domain size averaged over 10000 exciton generation events.

Figure 2 shows the fraction of dissociated excitons versus time for a variety of domain sizes and degrees of delocalization. In the ultra-fast temporal regime ($t < 1$ ps), for small domains (≤ 5 nm), nearly all excitons are dissociated at 10 nm of delocalization. With 1 and 5 nm delocalization, a small population of excitons is dissociated after localization. As the domain size is increased, fewer excitons are dissociated instantaneously across all three initial delocalization lengths. Additionally, for large domain sizes (20 nm), not all excitons are dissociated, corresponding to the exciton diffusion limit and reduced charge generation.

Note that these results reproduce the experimental findings of Figure 1C well, and comport with the reported morphologies of each material. For example, both Grancini et al. and Yamamoto et al. report for materials **1** and **2** in Figure 1, complete ultra-fast dissociation (< 1 ps) in their experiments, which is compatible with the high degree of mixing between the amorphous polymers and $PC_{60}BM$ acceptor in those materials systems. The large diffusion-limited component observed for the polymer:polymer system **5** also corresponds well to the large domain simulations, and at least partially explains the low quantum efficiencies reported to date for polymer:polymer blends.

In both experiment and this model, there is a significant exciton population that dissociates in < 1 ps, even in the absence of delocalization—in the largest domains, ca. 40% of excitons undergo dissociation before diffusion occurs. This effect arises solely from the large surface to volume ratio and the typically high fractal dimensionality of the domains. In our view, this raises the threshold at which exciton delocalization must be invoked, since geometric arguments alone plausibly explain up to 40% of the prompt exciton dissociation. In contrast, systems such as annealed P3HT:PC60BM exceed this threshold, and are thought to have sizable pure domains. In such systems, it is arguable that if ultra-fast exciton dissociation were solely the result of impure mixed domains, then poor collection features, not observed experimentally, would mark these devices.

As shown here, ultra-fast exciton dissociation in materials with sizable phase-pure domains is compatible with the initial delocalization of excitons. However, the simple geometric factor identified here, along with the possible presence of mixed domains, suggests that delocalization evidence based solely on prompt exciton dissociation requires heightened scrutiny. The initial delocalization potentially increases the exciton volumetric footprint, increasing the probability of reaching an interface in a delocalized state. If the exciton does not dissociate instantly, it then localizes and proceeds to diffuse in the donor material as described by traditional Förster energy transfer. As seen in the above experiments, larger domains correlate with diminished ultra-fast dissociation if the delocalization dimensions remain constant. Larger

initial delocalization yields a higher percentage of excitons dissociated in the ultra-fast time regime. The present methodology also makes it possible to calculate the effective delocalization of an exciton in a given material if the domain size of the BHJ donor material is known. This model enables the computation of delocalization lengths in materials and elucidation of structure-function relationships between materials structure and delocalization length.

It is not yet clear if exciton delocalization is ultimately essential for efficient exciton dissociation.[18] We note, for example, that several BHJ materials that exhibit a diffusion-limited component have also produced $>90\,\%$ internal device quantum efficiencies.[40–42] This result is incompatible with a differential outcome for the ultrafast and diffusion-limited populations of excitations. On the other hand, it seems difficult to explain the dissociation times by impure domains alone, since impure domains are also less favorable for charge collection.[25,26] Intercalating systems that stoichiometrically dissolve fullerenes along the polymer backbone provide an excellent illustration of the difficulty of extracting charge from an impure domain. These systems show little photocurrent generation and electron transport until sufficient acceptor is introduced to create a percolating domain.[43]

It is also important to avoid conflating the mechanism by which the excitation reaches the heterojunction with the mechanism of charge transfer. For example, here we have shown how excitations might access a heterojunction on the femtosecond timescale. However, this still leaves the actual mechanism of the ultrafast transfer unresolved. It is useful here to consider the literature on donor–bridge–acceptor chromophores which utilize structurally precise, covalently linked donor and acceptor molecules to study charge transfer. These systems guarantee contact between the donor and acceptor units, yet typically exhibit charge transfer on the order of picoseconds, significantly longer than the ultra-fast (<1 ps) charge transfer observed in BHJ blends.[44] A comparison between these two bodies of research suggests that the intimate contact provided by the BHJ alone is insufficient to explain the timescale of charge transfer.

In summary, a new model is proposed that reproduces the experimental exciton dissociation behavior of efficient BHJ OPVs. By combining the concept of initial exciton delocalization with Förster energy transfer, both the ultra-fast and slower dissociation processes can be incorporated in this model. The model reproduces experimental results, such as the diminished rapid dissociation with increasing domain size, and also lends insight into the interplay between mixed domains, domain geometry, and exciton delocalization. We show that up to 40 % of the ultrafast component can be explained by geometric factors alone. Additionally, the remaining ultrafast dissociation can be equivalently explained by impure domains or exciton delocalization. These results strongly suggest heightened experimental scrutiny of delocalization arguments based solely on pump–probe kinetic traces. When combined with transient absorption kinetics, the present model can predict the ratio of domain size to the effective exciton delocalization, providing further insight into the underlying OPV chemistry and physics, and suggests opportunities to measure the extent of delocalization for a given donor material.

Received: February 18, 2014
Published online: May 14, 2014

Keywords: donor–acceptor systems · energy transfer · FRET · molecular modeling · organic photovoltaics

[1] G. Li, R. Zhu, Y. Yang, *Nat. Photonics* **2012**, *6*, 153 – 161.
[2] T. M. Clarke, J. R. Durrant, *Chem. Rev.* **2010**, *110*, 6736 – 6767.
[3] C. W. Tang, *Appl. Phys. Lett.* **1986**, *48*, 183.
[4] G. Yu, J. Gao, J. C. Hummelen, F. Wudl, A. J. Heeger, *Science* **1995**, *270*, 1789 – 1791.
[5] S. R. Forrest, *MRS Bull.* **2005**, *30*, 28 – 32.
[6] S. M. Menke, W. A. Luhman, R. J. Holmes, *Nat. Mater.* **2013**, *12*, 152 – 157.
[7] R. C. Powell, Z. G. Soos, *J. Lumin.* **1975**, *11*, 1 – 45.
[8] T. Förster, *Radiat. Res. Suppl.* **1960**, *2*, 326 – 339.
[9] P. W. M. Blom, V. D. Mihailetchi, L. J. A. Koster, D. E. Markov, *Adv. Mater.* **2007**, *19*, 1551 – 1566.
[10] D. E. Markov, E. Amsterdam, P. W. M. Blom, A. B. Sieval, J. C. Hummelen, *J. Phys. Chem. A* **2005**, *109*, 5266 – 5274.
[11] S. R. Scully, M. D. McGehee, *J. Appl. Phys.* **2006**, *100*, 034907 – 034907.
[12] Z. He, C. Zhong, X. Huang, W.-Y. Wong, H. Wu, L. Chen, S. Su, Y. Cao, *Adv. Mater.* **2011**, *23*, 4636 – 4643.
[13] Y. Liang, Z. Xu, J. Xia, S.-T. Tsai, Y. Wu, G. Li, C. Ray, L. Yu, *Adv. Energy Mater.* **2010**, *22*, E135 – 8.
[14] X. Guo, N. Zhou, S. J. Lou, J. Smith, D. B. Tice, J. W. Hennek, R. P. Ortiz, J. T. L. Navarrete, S. Li, J. Strzalka, et al., *Nat. Photonics* **2013**, *7*, 825 – 833.
[15] I. A. Howard, R. Mauer, M. Meister, F. Laquai, *J. Am. Chem. Soc.* **2010**, *132*, 14866 – 14876.
[16] G. Grancini, M. Maiuri, D. Fazzi, A. Petrozza, *Nat. Mater.* **2012**, *12*, 29 – 33.
[17] L. G. Kaake, D. Moses, A. J. Heeger, *J. Phys. Chem. Lett.* **2013**, *4*, 2264 – 2268.
[18] S. Mukamel, *J. Phys. Chem. A* **2013**, *117*, 10563 – 10564.
[19] E. Collini, G. D. Scholes, *Science* **2009**, *323*, 369 – 373.
[20] F. Dubin, R. Melet, T. Barisien, R. Grousson, L. Legrand, M. Schott, V. Voliotis, *Nat. Phys.* **2005**, *2*, 32 – 35.
[21] S. Yamamoto, H. Ohkita, H. Benten, S. Ito, S. Yamamoto, D. Kitazawa, J. Tsukamoto, *J. Phys. Chem. C* **2013**, *117*, 11514 – 11521.
[22] J. M. Hodgkiss, A. R. Campbell, R. A. Marsh, A. Rao, S. Albert-Seifried, R. H. Friend, *Phys. Rev. Lett.* **2010**, *104*, 177701.
[23] P. Westacott, J. Tumbleston, S. Shoaee, S. Fearn, *Energy Environ. Sci.* **2013**, *6*, 2756 – 2764.
[24] B. A. Collins, J. R. Tumbleston, H. Ade, *J. Phys. Chem. Lett.* **2011**, *2*, 3135 – 3145.
[25] H. Chen, J. Peet, S. Hu, J. Azoulay, G. Bazan, M. Dadmun, *Adv. Funct. Mater.* **2013**, *24*, 140 – 150.
[26] W. Ma, J. R. Tumbleston, M. Wang, E. Gann, F. Huang, H. Ade, *Adv. Energy Mater.* **2013**, *3*, 864 – 872.
[27] A. F. Voter, *Radiation Effects in Solids*, Springer, Dordrecht, **2007**, pp. 1 – 23.
[28] H. Bässler, *Phys. Status Solidi B* **1993**, *175*, 15 – 56.
[29] G. Malliaras, R. Friend, *Phys. Today* **2005**, *58*, 53 – 58.
[30] B. J. Schwartz, *Annu. Rev. Phys. Chem.* **2003**, *54*, 141 – 172.
[31] I. Hwang, G. D. Scholes, *Chem. Mater.* **2011**, *23*, 610 – 620.
[32] M. M. L. Grage, P. W. Wood, A. Ruseckas, T. Pullerits, W. Mitchell, P. L. Burn, I. D. W. Samuel, V. Sundström, *J. Chem. Phys.* **2003**, *118*, 7644.

[33] K. Feron, W. Belcher, C. Fell, P. Dastoor, *Int. J. Mol. Sci.* **2012**, *13*, 17019 – 17047.
[34] B.-G. Kim, E. J. Jeong, J. W. Chung, S. Seo, B. Koo, J. Kim, *Nat. Mater.* **2013**, *12*, 659 – 664.
[35] P. K. Watkins, A. B. Walker, G. L. B. Verschoor, *Nano Lett.* **2005**, *5*, 1814 – 1818.
[36] B. C. Thompson, J. M. J. Fréchet, *Angew. Chem.* **2008**, *120*, 62 – 82; *Angew. Chem. Int. Ed.* **2008**, *47*, 58 – 77.
[37] C. R. McNeill, *Energy Environ. Sci.* **2012**, *5*, 5653 – 5667.
[38] E. Hennebicq, G. Pourtois, G. D. Scholes, L. M. Herz, D. M. Russell, C. Silva, S. Setayesh, A. C. Grimsdale, K. Müllen, J.-L. Brédas, et al., *J. Am. Chem. Soc.* **2005**, *127*, 4744 – 4762.
[39] A. A. Bakulin, A. Rao, V. G. Pavelyev, P. H. M. van Loosdrecht, M. S. Pshenichnikov, D. Niedzialek, J. Cornil, D. Beljonne, R. H. Friend, *Science* **2012**, *335*, 1340 – 1344.
[40] P. Schilinsky, C. Waldauf, C. J. Brabec, *Appl. Phys. Lett.* **2002**, *81*, 3885 – 3887.
[41] S. H. Park, A. Roy, S. Beaupré, S. Cho, N. Coates, J. S. Moon, D. Moses, M. Leclerc, K. Lee, A. J. Heeger, *Nat. Photonics* **2009**, *3*, 297 – 302.
[42] Y. Sun, G. C. Welch, W. L. Leong, C. J. Takacs, G. C. Bazan, A. J. Heeger, *Nat. Mater.* **2011**, *11*, 44 – 48.
[43] C. Bruner, N. C. Miller, M. D. McGehee, *Adv. Funct. Mater.* **2013**, *23*, 2863 – 2871.
[44] A. B. Ricks, G. C. Solomon, M. T. Colvin, A. M. Scott, K. Chen, M. A. Ratner, M. R. Wasielewski, *J. Am. Chem. Soc.* **2010**, *132*, 15427 – 15434.

